Volume 58, Number 6, June 2019

Molecular Carcinogenesis

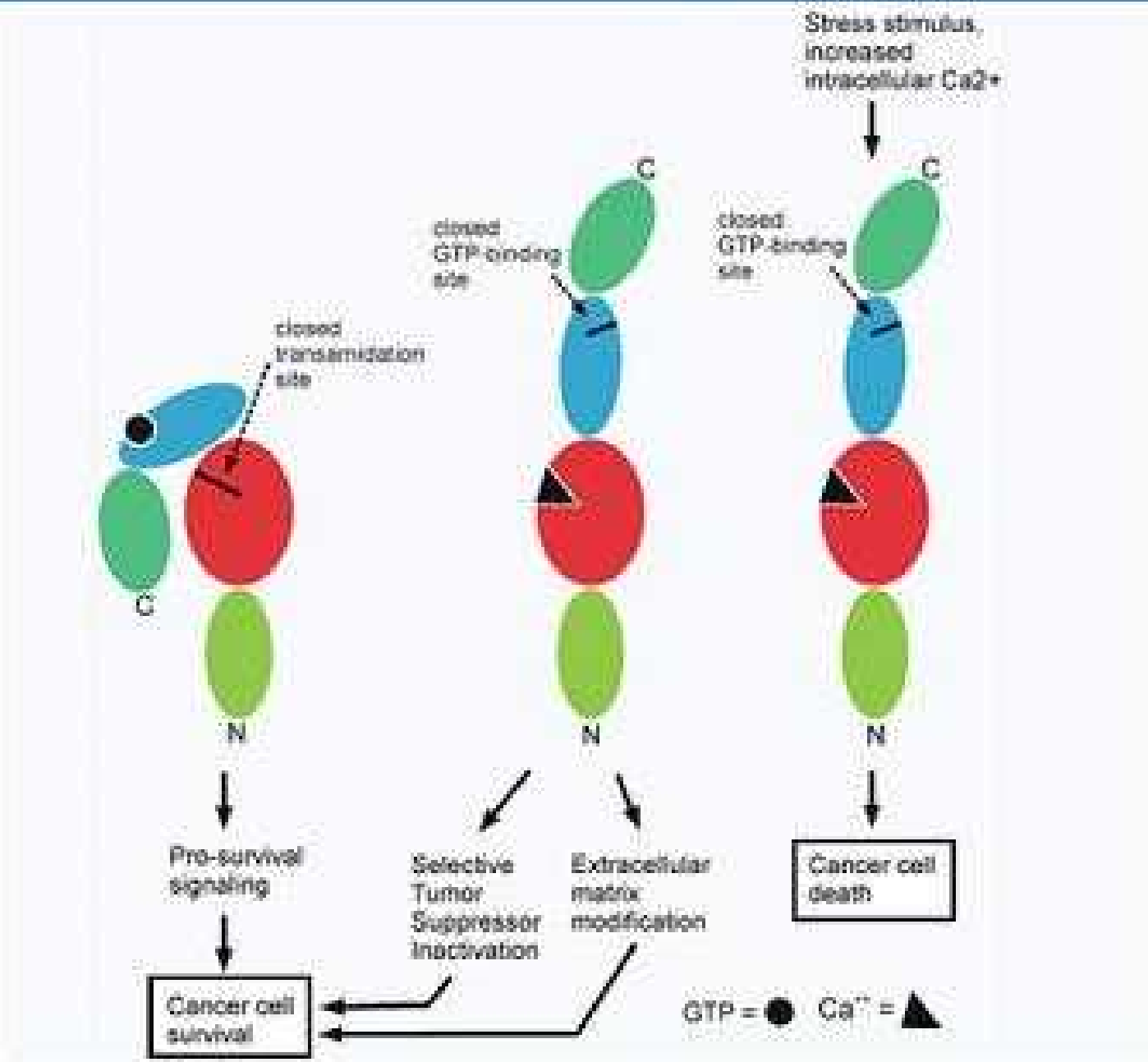

Editor-in-Chief Xiao-Jing Wang, MD, PhD

ISSN 0899-1987

WILEY

Molecular Carcinogenesis

Volume 58, Number 6, June 2019

Molecular Carcinogenesis

In This Issue

Continued on next page

WILEY

ISSN 0899-1987

Cover Caption: The cover image is based on the In Perspective *Transglutaminase 2 takes center stage as a cancer cell survival factor and therapy target* by Richard L. Eckert PhD, DOI 10.1002/mc.22986.

Received: 4 December 2018 | Revised: 28 January 2019 | Accepted: 29 January 2019
DOI: 10.1002/mc.22987

RESEARCH ARTICLE

WILEY Molecular Carcinogenesis

Neuroplastin-β mediates S100A8/A9-induced lung cancer disseminative progression

I Wayan Sumardika[1,2] | Youyi Chen[1] | Nahoko Tomonobu[1] | Rie Kinoshita[1] | I Made Winarsa Ruma[1,2] | Hiroki Sato[3] | Eisaku Kondo[4] | Yusuke Inoue[5] | Akira Yamauchi[6] | Hitoshi Murata[1] | Ken-ichi Yamamoto[1] | Shuta Tomida[7] | Kazuhiko Shien[3] | Hiromasa Yamamoto[3] | Junichi Soh[3] | Junichiro Futami[8] | Endy Widya Putranto[9] | Toshihiko Hibino[10] | Masahiro Nishibori[11] | Shinichi Toyooka[3] | Masakiyo Sakaguchi[1]

[1] Department of Cell Biology, Okayama University Graduate School of Medicine, Dentistry and Pharmaceutical Sciences, Okayama-shi, Okayama, Japan

[2] Faculty of Medicine, Udayana University, Denpasar, Bali, Indonesia

[3] Departments of Thoracic, Breast and Endocrinological Surgery, Okayama University Graduate School of Medicine, Dentistry and Pharmaceutical Sciences, Okayama-shi, Okayama, Japan

[4] Division of Molecular and Cellular Pathology, Niigata University Graduate School of Medicine and Dental Sciences, Niigata-shi, Niigata, Japan

[5] Faculty of Science and Technology, Division of Molecular Science, Gunma University, Kiryu-shi, Gunma, Japan

[6] Department of Biochemistry, Kawasaki Medical School, Kurashiki-shi, Okayama, Japan

[7] Department of Biobank, Okayama University Graduate School of Medicine, Dentistry and Pharmaceutical Sciences, Kita-ku, Okayama, Japan

[8] Department of Medical and Bioengineering Science, Okayama University Graduate School of Natural Science and Technology, Kita-ku, Okayama, Japan

Compiling evidence indicates an unusual role of extracellular S100A8/A9 in cancer metastasis. S100A8/A9 secreted from either cancer cells or normal cells including epithelial and inflammatory cells stimulates cancer cells through S100A8/A9 sensor receptors in an autocrine or paracrine manner, leading to cancer cell metastatic progression. We previously reported a novel S100A8/A9 receptor, neuroplastin-β (NPTNβ), which plays a critical role in atopic dermatitis when it is highly activated in keratinocytes by an excess amount of extracellular S100A8/A9 in the inflammatory skin lesion. Interestingly, our expression profiling of NPTNβ showed significantly high expression levels in lung cancer cell lines in a consistent manner. We hence aimed to determine the significance of NPTNβ as an S100A8/A9 receptor in lung cancer. Our results showed that NPTNβ has strong ability to induce cancer-related cellular events, including anchorage-independent growth, motility and invasiveness, in lung cancer cells in response to extracellular S100A8/A9, eventually leading to the expression of a cancer disseminative phenotype in lung tissue in vivo. Mechanistic investigation revealed that binding of S100A8/A9 to NPTNβ mediates activation of NFIA and NFIB and following SPDEF transcription factors through orchestrated upstream signals from TRAF2 and RAS, which is linked to anchorage-independent growth, motility and invasiveness. Overall, our results indicate the importance of the S100A8/A9-NPTNβ axis in lung cancer disseminative progression and reveal a pivotal role of its newly identified downstream signaling, TRAF2/RAS-NFIA/NFIB-SPDEF, in linking to the aggressive development of lung cancers.

Abbreviation: ALCAM, Activated leukocyte cell adhesion molecule; ASS1, Argininosuccinate Synthase 1; CDP, CCAAT-displacement protein; DKK1, Dickkopf WNT Signaling Pathway Inhibitor 1; EGFR, Epidermal growth factor receptor; EMMPRIN, Extracellular matrix metalloproteinase inducer; ERAS, Embryonic Stem Cell-Expressed Ras; ERBB2, Erb-B2 receptor tyrosine kinase 2; EMSA, Electrophoretic mobility shift assay; FAST1, Forkhead Activin Signal Transducer-1; FTS, Farnesyl Thiosalicylic Acid; GRB2, Growth Factor Receptor Bound Protein 2; HSF, Heat shock transcription factors; ID4, Inhibitor of DNA Binding 4; IDH1, Isocitrate Dehydrogenase [NADP] Cytoplasmic 1; KLF4, Kruppel Like Factor 4; KLF13, Kruppel Like Factor 13; MCAM, Melanoma cell adhesion molecule; NF, Nuclear Factor; NPTN, Neuroplastin; RAGE, Receptor for advanced glycation endproducts; RASL11A, RAS-Like Family 11 Member A; SPDEF, SAM pointed-domain containing ETS transcription factor; SSSRs, S100-soil signal receptors; THBS1, Thrombospondin 1; TLR4, Toll-like receptor 4; TRAF2, TNF receptor associated factor 2.

Toshihiko Hibino passed away on Jun 1 in 2016.

[9] Department of Pediatrics, Dr. Sardjito Hospital/Faculty of Medicine, Universitas Gadjah Mada, Yogyakarta, Indonesia

[10] Department of Dermatology, Tokyo Medical University, Shinjuku-ku, Tokyo, Japan

[11] Department of Pharmacology, Okayama University Graduate School of Medicine, Dentistry and Pharmaceutical Sciences, Okayama-shi, Okayama, Japan

Correspondence
Masakiyo Sakaguchi, PhD, Department of Cell Biology, Okayama University Graduate School of Medicine, Dentistry and Pharmaceutical Sciences, 2-5-1 Shikata-cho, Kita-ku, Okayama-shi, Okayama 700-8558, Japan.
Email: masa-s@md.okayama-u.ac.jp

Funding information
the Project for Cancer Research and Therapeutic Evolution (P-CREATE) from the Japan Agency for Medical Research and Development (AMED), Grant number: JP17cm0106216; Takeda Science Foundation; JSPS KAKENHI, Grant number: 17H03577; Princess Takamatsu Cancer Research Fund; Kobayashi Foundation for Cancer Research; Fujii Memorial Medical Science Foundation

KEYWORDS
lung cancer, NFI, NPTNβ, S100 protein, S100A8/A9, SPDEF

1 | INTRODUCTION

Lung cancer is one of the problematic cancer diseases leading to cancer death because of an early onset of metastatic dissemination.[1] It is known that lung cancer cells readily obtain metastatic ability, but the related molecular mechanism(s) is unclear and the factors that change cells into an aggressive phenotype remain poorly understood.

The secretory molecule S100A8/A9, which is a heterodimer complex of S100A8 and S100A9 proteins, recently getting more attention as a factor on cancer metastasis. When cancer cells are present in a remote area, cancer-related inflammation occurs in sensitive lung tissue by recognizing abnormalities caused by the cancer cell behaviors, where the recruited immune cells produce a large amount of S100A8/A9.[2] This phenomenon is linked to the formation of a pre-metastatic immunosuppressive environment and acts on chemotactic attraction of the remote cancer cells to the lung area.[2,3] It has been reported that toll-like receptor 4 (TLR4) and receptor for advanced glycation end products (RAGE) behave as receptors for S100A8/A9.[4–8] However, it is hard to explain the S100A8/A9-related metastatic phenomena in a variety of cancer cells by only two types of receptors.

We therefore tried to find other candidate receptors for S100A8/A9, and we succeeded in the identification of novel receptors, extracellular matrix metalloproteinase inducer (EMMPRIN),[9] melanoma cell adhesion molecule (MCAM),[10,11] activated leukocyte cell adhesion molecule (ALCAM)[10] and neuroplastin (NPTN)-α and -β,[12] which we termed as S100-soil signal receptors (SSSRs).[10,11] Interestingly, EMMPRIN, which is highly expressed in metastatic melanoma cells, binds specifically to the S100A9 side of S100A8/A9, and it was shown that the binding caused melanoma metastasis to artificially S100A9-overexpressed skin tissue.[9] MCAM and ALCAM are also positively at high levels expressed in melanoma cells and play a role in the migration of melanoma cells toward S100A8/A9-expressed lung tissue.[10] We found that NPTN, especially in its beta isoform (NPTNβ), is dominantly expressed in skin keratinocytes and can bind with both the S100A8 and S100A9 sides of the S100A8/A9 heterodimer complex and that binding has a critical role in skin hyperplasia in atopic dermatitis.[12] Although we found a significant role of NPTNβ in keratinocytes, its specific role in cancer has remained to be clarified.

It has long been recognized that extracellular S100A8/A9 plays a pivotal role in cancer progression through certain cell surface receptors.[4–10] Induction and secretion of the protein closely associated with several inflammatory settings including a cancer-mediated inflammatory setting.[4–11] Accumulating evidence indicates that induction of S100A8/A9 at a significant level readily occurs in lung tissue even when cancer cells appear in a region distant from the lung and that the induction of S100A8/A9 results in lung metastasis of cancer cells and their subsequent development in the inflammatory lung.[8,13] That evidence suggests that lung cancer may be greatly affected by just surrounding S100A8/A9, which is linked to the acquisition of a malignant phenotype in cancer cells in a short period of time. If so, lung cancer cells require a certain receptor to accept the S100A8/A9 signal in an efficient manner.

In this study, we investigated unidentified functions of NPTNβ in cancer cells. First, we investigated the expression level of NPTNβ in lung cancer, the protein was commonly expressed at a high level in lung cancer cells, leading us to focus on the role of the protein in lung cancer. Considering the association between S100A8/A9 and NPTNβ in the lung cancer microenvironment, we hypothesized that S100A8/A9 might induce lung cancer progression. We found that NPTNβ-overexpressed lung cancer cells change an aggressive phenotype in response to S100A8/A9 both in vitro and in vivo in a mouse model. The S100A8/A9-NPTNβ binding event leads to significant activation of the NFI transcription factors NFIA and NFIB and SAM pointed-domain containing ETS transcription factor (SPDEF), eventually leading to the appearance of an aggressive phenotype in lung cancer cells. Collectively, our findings suggest that the S100A8/A9-NPTNβ signaling axis plays a significant role in the promotion of lung cancer with acquisition of metastatic traits.

2 | MATERIALS AND METHODS

We used HEK293T (human embryonic kidney cell line stably expressing the SV40 large T antigen; RIKEN BioResource Center, Tsukuba, Japan), the non-cancerous immortalized human bronchial epithelial cell line BEAS-2B (ATCC, Rockville, MD) and the human lung cancer cell line A549 (*KRAS*-mutant: G12S; ATCC). All cells were cultivated in D/F medium (Thermo Fisher Scientific, Waltham, MA) supplemented with 10% FBS at 37.0°C with 5% CO_2. A mutant KRAS inhibitor, K-Ras (G12C) Inhibitor 12 (10 μM, Cayman Chemical, Ann Arbor, MI), and a pan-RAS inhibitor, Farnesyl Thiosalicylic Acid (FTS 50 μM, Cayman Chemical), were used to inhibit intracellular RAS function in A549 cells.

Human S100A8/A9 recombinant protein was expressed in HEK293 cells using the FreeStyle 293 Expression System (Thermo Fisher Scientific) as previously reported.[10] The secreted S100A8/A9 was then purified by Talon® Metal affinity resin (Takara Bio, Shiga, Japan). exNPTNβ-Fc was prepared as described previously.[12]

For temporal expression, we used the pIDT-SMART (C-TSC) vector, also named pCMViR-TSC, as previously reported.[14] A series of cDNAs was inserted into pIDT-SMART (C-TSC). The inserted cDNAs were human cDNAs encoding NPTNβ, NPTNβ dn (deletion of the cytoplasmic tail: Δ 361-398 aa), NFIA, NFIB, NFIC, NFIX, NFIA dn (deletion of the N-terminal DNA-binding domain: Δ 1-194 aa), NFIB dn (deletion of the N-terminal DNA-binding domain: Δ 1-195 aa), TRAF2 dn (deletion of the N-terminal domain: Δ 1-85 aa). NPTNβ wt and NPTNβ dn were designed for expression as C-terminal 3xHA-6His-tagged forms. NFIA, NFIB, NFIC, NFIX, NFIA dn, NFIB dn, and TRAF2 dn were designed for expression as C-terminal Myc-6His-tagged forms. Cells were transiently transfected with the plasmid vectors using FuGENE-HD (Promega, Madison, WI).

We also established several A549 stable clones that showed indefinitely stable expression of the aberrant genes of interest at much higher levels. Based on the pIDT-SMART (C-TSC) vector, we made two improved vectors for stable expression with significantly higher level, named pSAKA-1B[14] and pSAKA-4B.[11] The expression vector pSAKA-1B is specifically adapted to Chinese hamster ovary (CHO) cells, while pSAKA-4B is useful for a wide range of diverse cell lines from different kinds of mammalian species in a constant manner. A549-originated clones (see Figure S4) were established by a convenient electroporation gene delivery method using pSAKA-4B and subsequent selection with puromycine at 20 μg/mL.

Quantitative real-time PCR was performed as described previously.[10,11] A LightCycler rapid thermal cycler system (ABI 7900HT; Applied Biosystems, Foster City, CA) was run using LightCycler 480 SYBR Green I Master (Roche Diagnostics, Indianapolis, IN) according to the manufacturer's instructions. Forward and reverse primer pairs used (5′ to 3′) are listed in Table S2. The amounts of mRNA were calibrated to those of TBP and are presented as ratios to those of the indicated controls.

Pre-designed siRNAs for human NPTN (#1, ID No. s25707; #2, s25708), NFIA (#1, ID No. s9476; #2, ID No. s9477; #3, ID No. s9478), SPDEF (#1, ID No. s24518; #2, ID No. s24519; #3, ID No. s195114) and control siRNA (Silencer Negative control two siRNA) were purchased from Thermo Fisher Scientific. Decoy DNAs for TFs, CDP, FAST1, NFI and HSF, were prepared by hybridizing primer pairs corresponding to each TF. The primer sequences are shown in Table S1. siRNAs and decoy DNAs were transfected using Lipofectamin RNAiMAX reagent (Thermo Fisher Scientific).

Western blotting was performed under conventional conditions. The antibodies used were as follows: mouse anti-HA tag antibody (Cell Signaling Technology, Beverly, MA), mouse anti-Myc antibody (Cell Signaling Technology), mouse NFI (NFIA) antibody (Santa Cruz Biotechnology, Santa Cruz, CA), rabbit anti-NFIB antibody (Proteintech, Rosemont, IL), rabbit anti-NFIC antibody (Proteintech), rabbit anti-NFIX (Proteintech), rabbit anti-SPDEF antibody (Proteintech) and mouse anti-β-actin antibody (Sigma-Aldrich). The second antibody was horseradish peroxidase-conjugated anti-mouse antibody (Cell Signaling Technology). Positive signals were detected by a chemiluminescence system (ECL plus, GE Healthcare Bio-Sciences, Piscataway, NJ).

Paraffin-embedded sections from human lung cancer tissues were deparaffinized, and antigen retrieval was performed by conventional trypsin treatment. Endogenous peroxide activity was quenched by treatment of the specimens with 3% hydrogen peroxide (Kanto Chemical Co., Inc, Hokkaido, Japan) for 10 min at room temperature (RT). Slides were incubated overnight at 4°C with either rabbit anti-NPTN antibody (Sigma-Aldrich, St Louis, MO) or mouse anti-Calprotectin (S100A8/A9) antibody (Hycult Biotech, Plymouth Meeting, PA). After washing the slides with 0.05% Tween-20 in PBS, the slides were incubated with a horseradish peroxidase (HRP)-labeled secondary antibody. Signal detection was performed by treatment of the antibody-reacted slides with a substrate, 3-amino-9-ethylcarbazole (AEC) (HISTOFINE simple stain AEC solution, Nichirei Biosciences, Tokyo, Japan).

Comprehensive analysis of transcription factors (TFs) that are activated by NPTNβ was performed by using protein/DNA array I (Thermo Fisher Scientific) according to the manufacturer's instructions. Nuclear extracts from HEK293T cells with either expression of GFP or NPTNβ were prepared using NE-PER Nuclear and Cytoplasmic

Extraction Reagents (Thermo Fisher Scientific) and were applied to the array. Nuclear extracts from A549 cells were also prepared by the same method, and EMSA was performed using the LightShift Chemiluminescent EMSA kit (Thermo Fisher Scientific). A 5′-biotin-labeled double-stranded probe (Forward: 5′-gaaTTGGCaacttGCCAAcga-3′; Reverse: 3′-tcgTTGGCaagttGCCAAttc-5′) was purchased from Sigma-Aldrich. For super shift analysis, an anti-NFIA antibody (condensed to 10-fold) (Santa Cruz Biotechnology, Santa Cruz, CA) was added to the reaction mixture containing the probe and nuclear extract, and the mixture was further incubated on ice for 10 min. DNA-protein complexes were fractionated by 7% PAGE and blotted onto a Biodyne B nylon membrane (Pall, Tokyo, Japan).

Cells were starved by serum-free D/F medium for 24 h prior to invasion and migration assays. Cell invasion or migration was assayed using the Boyden chamber method with filter inserts (pore size, 8 μm) pre-coated or not pre-coated with Matrigel in 24-well plates (BD Biosciences, Franklin Lakes, NJ). Cells (3×10^4 cells/insert) were seeded with serum-free D/F medium on the top chamber, the bottom chamber was filled with D/F medium containing 10% FBS. The recombinant S100A8/A9 was then set in the bottom chamber at a final concentration of 10, 100, or 1000 ng/mL. After incubation for 12 h, cells that passed through the filter were counted by staining with 0.01% crystal violet in 25% methanol. Migrated/invaded cells were quantified by cell counting in five non-overlapping fields at ×100 magnification and are presented as the average from three independent experiments.

The cell growth condition in a culture dish was evaluated by using the Cell-Titer-Glo™ Luminescent Cell Viability assay kit (Promega). The luminescence was determined by a Fluoroskan Ascent FL luminometer (Thermo Fisher Scientific). The chambers in 6-well plates were coated with 1 mL of 0.8% agarose medium. Cells (1×10^4 cells in 1 mL 0.4% agarose medium) were seeded on top of the base agar, after 30 min the chambers were filled with 1 mL D/F medium + 10% FBS with or without 1000 ng/mL of recombinant S100A8/A9. The medium was refreshed every 3 days. After 14 days of incubation, the colonies were counted by staining with 0.01% crystal violet in 25% methanol. Colonies that were more than 50 μm in size were then quantified in five non-overlapping fields at ×100 magnification and are presented as the average from three independent experiments.

Six-week-old female nude mice, BALB/c-nu mice, were purchased from Charles River Laboratories (Yokohama, Japan). All mice were provided with sterilized food and water and were housed in a barrier facility under a 12:12-h light/dark cycle. A549 cells and their derivatives (5×10^5 cells in 0.1 mL PBS/mouse) were injected into the lungs of each mouse. One month after injection, the tumor nodules in the whole lung was observed by LaTheta® X-ray computed tomography (CT-scan, Hitachi-Aloka Medical, Tokyo, Japan) and the lungs and other organs were isolated and analyzed microscopically.

All values are expressed as means ± SD. All data were analyzed by the unpaired Student's *t*-test for significant differences between the mean values of each group.

3 | RESULTS

3.1 | NPTN and S100A8/A9 are highly expressed in lung cancer

Besides classical S100A8/A9 receptors, toll-like receptor 4 (TLR4)[4,5] and receptor for advanced glycation end products (RAGE),[5,6] we have reported the presence of the important novel receptors including extracellular matrix metalloproteinase inducer (EMMPRIN), neuroplastin (NPTN)α and β, melanoma cell adhesion molecule (MCAM) and activated leukocyte cell adhesion molecule (ALCAM).[7–12] Among these receptors, we found that lung cancer cell lines highly express NPTNβ compared with normal cells lines (Figure S1A). This finding was supported by the result of immunohistochemistry showing that NPTNβ was highly positive in lung cancer cells and that S100A8/A9 appeared in either cancer cells or the surrounding stroma in clinical specimens, suggesting that extracellular S100A8/A9 physiologically acts on cell surface NPTNβ in cancer cells in an autocrine manner as well as a paracrine manner (Figure 1). The immunohistochemistry also showed that the expression of NPTN was much higher in lung cancer cells compared with those in non-neoplastic counterparts (Figure S1B). In order to further investigate clinical significance of different expression of NPTN and S100A8/9 in survival of lung cancer patients, we used publicly available data set[15] of the SurvExpress database[16] (http://bioinformatica.mty.itesm.mx:8080/Biomatec/SurvivaX.jsp) and analyzed the issue. Correlative studies between expression levels of these proteins and clinical outcomes resulted in significantly decrease in overall survival of patients with high level of NPTN (Figure S2A, S2B and S2C). This tendency was not observed in lung cancer patients with high level of either S100A8 or S100A9. These results suggest an unusual role of NPTN in lung cancer progression to malignant stages. We therefore decided to investigate the biological significance of the S100A8/A9-NPTNβ signaling axis in lung cancer progression.

3.2 | NPTNβ-mediated cellular events in response to S100A8/A9

To get an insight into the function of NPTNβ in response to S100A8/A9 in lung cancer cells, we did in vitro experiment to evaluate the cancer characteristics in A549 cells. Forced expression of NPTNβ resulted in a slight increase in the growth of A549 cells and S100A8/A9 at concentrations of 10 to 1000 ng/mL did not stimulate growth of the cells in either MTS-based evaluation (Figure 2A) or EdU uptake assay (data not shown). In addition, overexpression of NPTNβ and/or stimulation of S100A8/A9 did not show any appreciable elevation of apoptotic cells in the stimulated A549 cells as we found by Annexin V staining (data not shown). Meanwhile, a three-dimensional soft agar assay showed that overexpression of NPTNβ induced significant anchorage-independent growth of A549 cells and that the growth was further enhanced by S100A8/A9 treatment in a dose-dependent manner (Figure 2B). We also found that S100A8/A9-induced migration and invasion were both promoted by

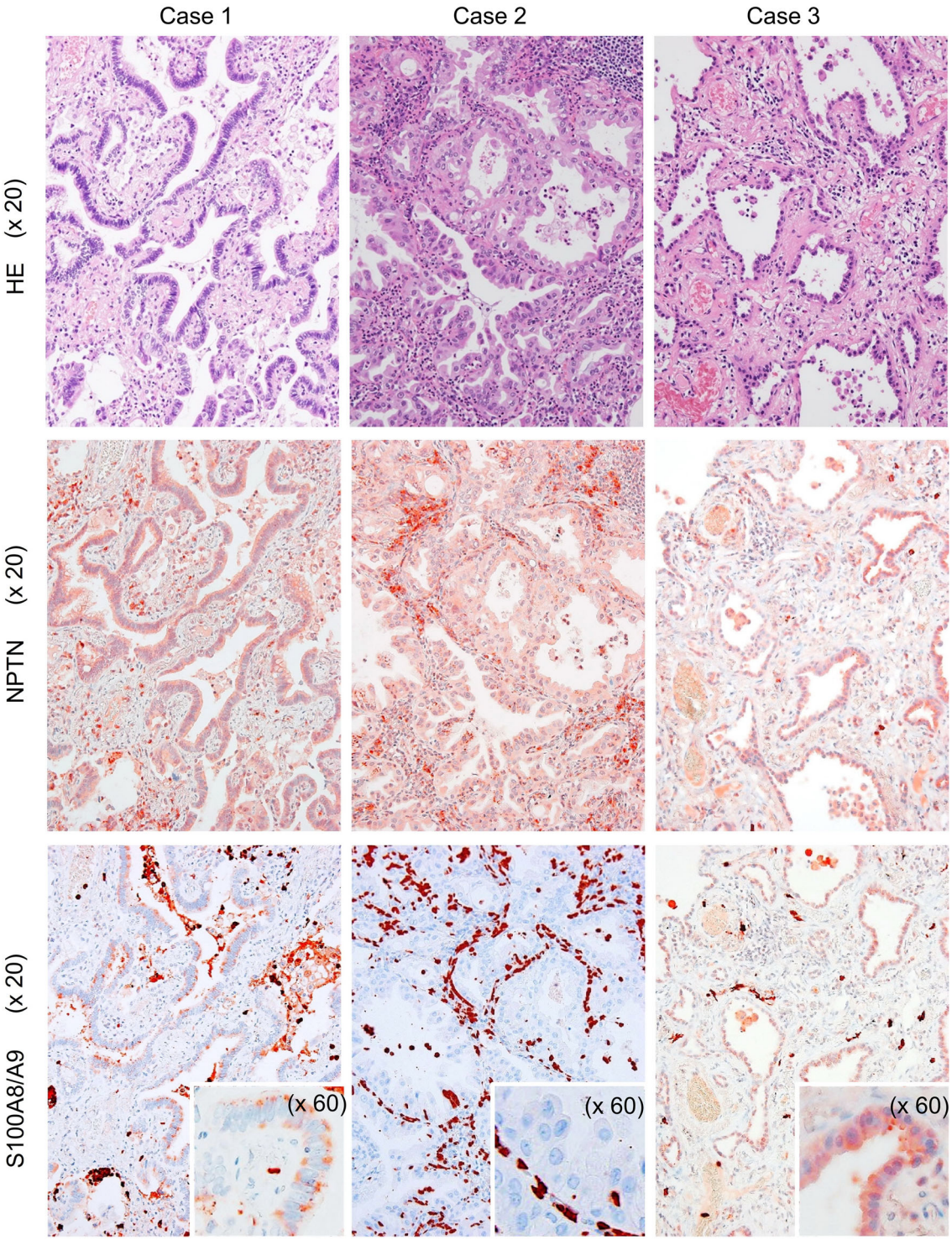

FIGURE 1 Distribution patterns of NPTNβ and S100A8/A9 in lung cancers prepared from lung cancer patients. Expression and localization of NPTNβ and S100A8/A9 were detected in indicated lung lesions including stroma areas in an ordinal view (×20). Insets: stretched view (×60). [Color figure can be viewed at wileyonlinelibrary.com]

NPTNβ overexpression (Figures 2C and 2D). The optimal concentrations of S100A8/A9 were 1000 ng/mL for anchorage-independent growth, 10 ng/mL for chemotaxis, and 1000 ng/mL for invasion. To confirm the results, we then blocked the function of intrinsic NPTNβ in A549 cells by forced expression of cytoplasmic tail-deficient NPTNβ (NPTNβ dn). The result showed that the S100A8/A9-mediated cancer behaviors were abolished by this approach (Figures S3A, S3B, S3C). To strengthen the results, we next used siRNA to knock down the endogenous NPTNβ in A549 cells and evaluated the same cellular events under the presence or absence of extracellular S100A8/A9. Within our expectation, knockdown of NPTNβ removed the cancer-associated abilities of

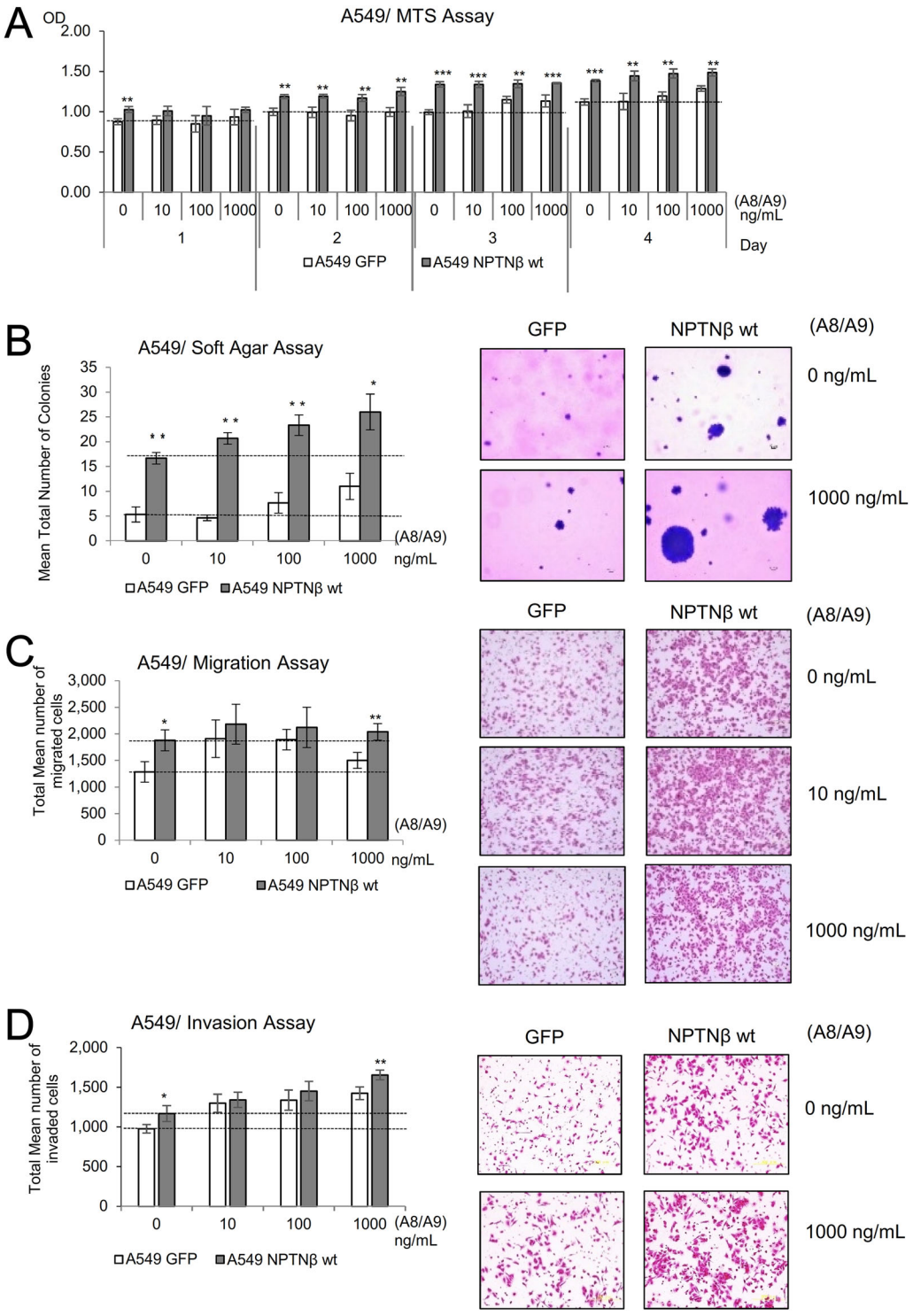

FIGURE 2 NPTNβ-mediated cellular events in response to S100A8/A9. A, A549 cells were transfected with either GFP as a control or NPTNβ expression vector and then treated with S100A8/A9 (10-1000 ng/mL) during the indicated days. Cell growth of each sample was evaluated on different days by MTS assay. B, Anchorage-independent growth was assessed in A549 cells in floating culture filled with 0.4% agarose-containing medium. A549 cells with temporal overexpression of foreign GFP or NPTNβ were treated or not treated with 10–1000 ng/mL S100A8/A9 for two weeks, and evaluation was carried out by counting the formed spheroids exceeding 50 μm in size. Right panel shows representative images of the spheroids. C, D, Effects of NPTNβ overexpression on S100A8/A9-induced migration and invasion. Migration (C) and invasion (D) of A549 cells transfected with the indicated gene (GFP as a control or NPTNβ) were assessed by the Boyden chamber method. The transfected A549 cells were placed in the top chamber and purified recombinant S100A8/A9 (10–1000 ng/mL) was added to the bottom well. Quantified results are displayed in the left parts and representative images of migrating cells detected by crystal violet staining are shown in the right parts. Data from A through D are means ± SD, $^{*}P < 0.05$ and $^{**}P < 0.01$. [Color figure can be viewed at wileyonlinelibrary.com]

anchorage independent growth, migration and invasion from A549 cells even after stimulation with S100A8/A9 (Figures S3D, S3E, S3F). These results together with the results shown in Figure 1 suggest that cell surface S100A8/A9-NPTNβ interaction has an important role in lung cancer progression.

3.3 | Critical function of NFIA and NFIB in S100A8/A9-NPTNβ-mediated cellular events

We next addressed NPTNβ downstream signaling, which plays a central role in the S100A8/A9-mediated cellular events. Activation profiling of transcription factors (TFs) revealed several candidates that were activated by NPTNβ (Figure 3A). Among these, we were interested in CDP, FAST1, NFI and HSF. To narrow down the number of candidates, we transfected TF-targeting cis-DNA elements as decoys (Table S1) to inhibit the function of each TF in cells. We performed forced expression of NPTNβ as well as transduction of decoy DNAs in BEAS-2B cell line because it has lower expression level of intrinsic NPTNβ than A549 cells (Figure S1A). As shown in Figure 3B, we found that all the decoys had the ability to mitigate NPTNβ-induced migration, the greatest inhibition was observed when we used an NFI decoy (left panel). Assessment of growth in the same cells showed almost the same tendency as that for migration (middle panel). However, only the NFI decoy had a suppressive effect on the growth of A549 cells (right panel), and we therefore decided to focus on NFI. Since the NFI family is composed of four proteins, we examined the expression levels of these proteins in lung cancer cell lines and found that NFIA showed a higher expression level in cancer cells than in immortalized BEAS-2B cells (Figures 3C and 3D). Unexpectedly, other NFI family proteins showed lower expressions levels in cancer cell lines than in BEAS-2B cells. However, by cell-based assay we found the significance of NFIA and NFIB, but not NFIC and NFIX, in S100A8/A9-NPTNβ-mediated migration and invasion (Figures 3E and 3F).

To confirm the results obtained for NFIA and NFIB, we newly constructed NFIA dn and NFIB dn that lack DNA-binding domains. After transfection of the indicated plasmids, we found that growth activity was significantly downregulated in NFIA dn or NFIB dn-transduced cells compared to that in wild-types cells (Figure 4A). In addition, both NFIA dn and NFIB dn reduced basal activities of cancer-related cellular behaviors, including anchorage-independent growth (Figure 4B), migration (Figure 4C) and invasion (Figure 4D), even under the condition with S100A8/A9 stimulation. Interestingly, our immunoprecipitation results showed that NFIA and NFIB are able to form homodimer or/and heterodimer, in which DNA binding domains were not required for the dimerization since both NFIA dn and NFIB dn are able to bind to full length of NFIA (Figure 4E, left panel). Regarding to this, either NFIA dn or NFIB dn significantly attenuated NFIA function to bind its target DNA sequence (Figure 4E, right panel), suggesting that NFIA needs either NFIA as homodimer or NFIB as heterodimer for its transcriptional activation.

Evaluation using siRNA was further performed to reinforce the results as described above. Similarly, to the effects of dominant negative NFIA, the anchorage independent growth, migration and invasion abilities of A549 cells were also greatly reduced by the NFIA siRNAs, even in the condition of S100A8/A9 stimulation (Figure S4A-S4D). An electrophoretic mobility shift assay (EMSA) revealed that activation of NFIA was immediately occurred and highest activation was occurred at 6 h in response to S100A8/A9 stimulation (Figure 4F, left and middle panels), and NPTNβ was required for this reaction in A549 cells since S100A8/A9-induced NFIA activation was significantly reduced by NPTNβ dn forced expression as well as by NPTN siRNA transduction (Figure 4F, right panel).

Interestingly, the transfection experiments shown that temporal expression of NPTNβ wt, NFIA and NFIB induced a mesenchymal stromal cell-like shape in A549 cells (data not shown). This morphological change was also obvious when sublines were established from A549 parental cells (Figure S5A). Stable clones over-expressing either NPTNβ wt alone or NPTNβ wt + (NFIA wt + NFIB wt) displayed a sparsely distributed phenotype, while such a character was lost in the established sublines of NPTNβ wt + (NFIA dn + NFIB dn) (Figure S5B). These observations suggested that the S100A8/A9-NPTNβ-NFI signaling axis upregulates cellular motility, which is crucial in cancer progression. To examine this possibility, we further assessed the characteristics of the established clones (Figure S6A, migration; Figure S6B, invasion; Figure S6C, spheroidal formation). Interestingly, NPTNβ stable transformant clones #10, 11, 12, 18, 23, 24 showed higher activities for migration, invasion and spheroid formation in response to S100A8/A9 than the activities shown by the control GFP transformant (left panels). The stable transformant NPTNβ wt + (NFIA wt + NFIB wt) clones #1, 2, 4, 5, 12, 15 also showed a tendency for enhancement of activities by S100A8/A9 stimulation (middle panels). On the other hand, these cellular activities in response to extracellular S100A8/A9 stimulation were all homogeneously diminished in the stable transformant of NPTNβ wt + (NFIA dn + NFIB dn) clones #1, 2, 3, 7, 10, 24 (right panels). These results obtained by using stable clones as well as the results obtained with temporal expression suggest that the newly identified S100A8/A9-NPTNβ-NFIA/NFIB pathway has a critical role in certain lung cancer progression.

3.4 | NFIA/NFIB-mediated induction of SPDEF promotes cellular spheroidal growth, migration and invasion

To examine downstream molecules relevant to cancer progression for which expression is regulated by the S100A8/A9-NPTNβ-NFIA/NFIB pathway, we performed comprehensive gene expression analysis using RNA sequencing. In this analysis, we compared the gene expression profiles of the control GFP clone and NPTNβ wt + NFIA wt + NFIB wt clone #12 and gene expression profiles of the control GFP clone and NPTNβ wt + NFIA dn + NFIB dn clone #2 since our aim was to identify genes with altered expression that showed an inverse relation between wt and dn of NFIA/NFIB under the condition of NPTNβ wt over-expression. First, we classified genes with altered expression according to the DISEASE category (Figure S7A). The number of genes with altered expression that are associated with PHARMACOGENOMICS was largest in the disease category, followed by genes associated with CARDIOVASCULAR, OTHER, METABOLIC, CANCER and

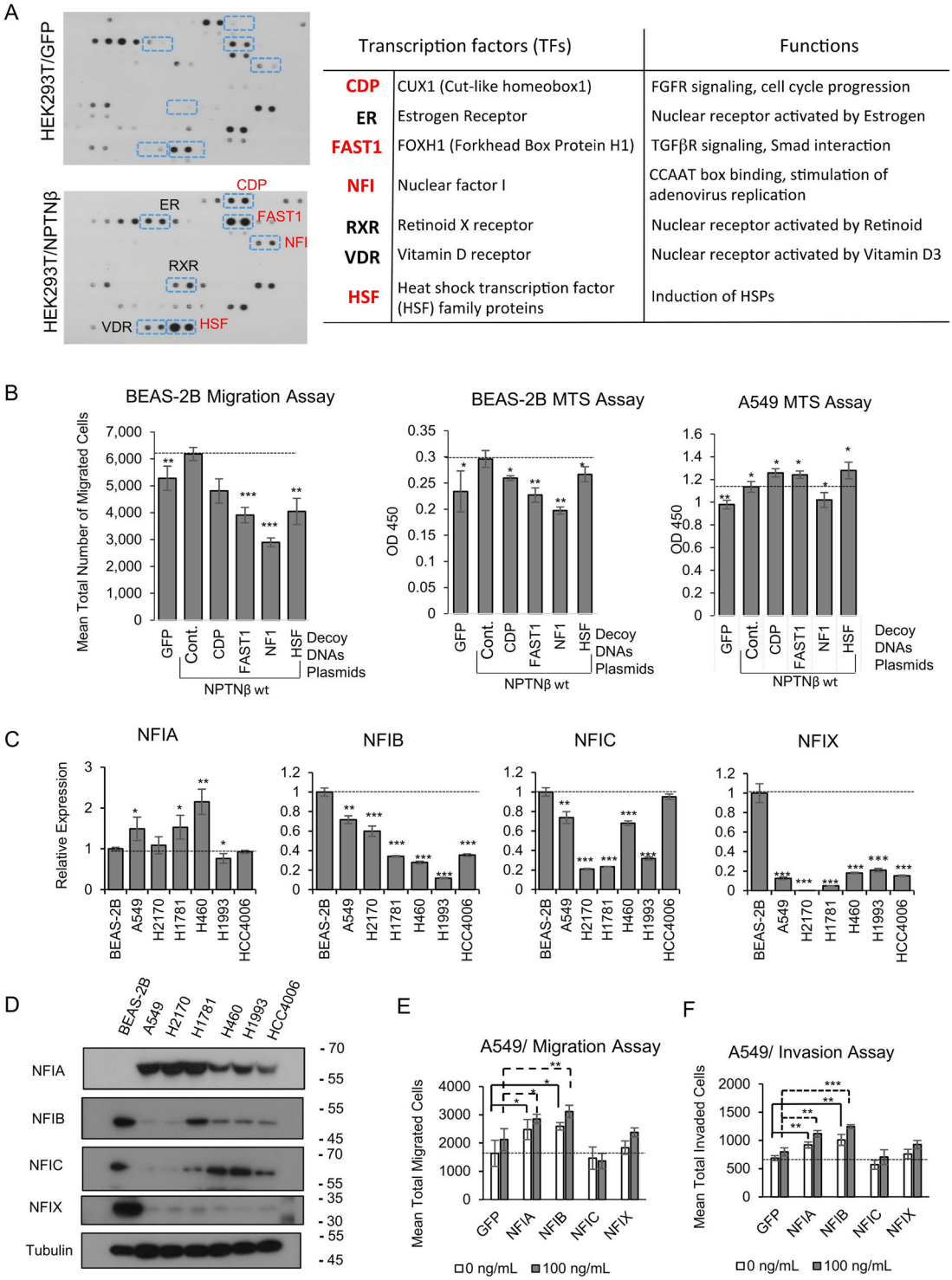

Transcription factors (TFs)		Functions
CDP	CUX1 (Cut-like homeobox1)	FGFR signaling, cell cycle progression
ER	Estrogen Receptor	Nuclear receptor activated by Estrogen
FAST1	FOXH1 (Forkhead Box Protein H1)	TGFβR signaling, Smad interaction
NFI	Nuclear factor I	CCAAT box binding, stimulation of adenovirus replication
RXR	Retinoid X receptor	Nuclear receptor activated by Retinoid
VDR	Vitamin D receptor	Nuclear receptor activated by Vitamin D3
HSF	Heat shock transcription factor (HSF) family proteins	Induction of HSPs

FIGURE 3 Screening of a significant transcription factor(s) for S100A8/A9-NPTNβ-mediated cellular events. A, GFP or NPTNβ was temporally expressed in HEK293 cells and then activated transcription factors for their nuclear extracts prepared using a screening array membrane were analyzed. B, BEAS-2B cells were co-transfected with an NPTNβ plasmid and the indicated decoy DNA fragments (0.1 μM) and subjected to the Boyden chamber-based migration assay (left). Similarly, cell growth was evaluated 48 h after co-transfection with them in BEAS-2B cells (middle) and A549 cells (right). C, Expression profiling of NFI family genes. Total RNAs prepared from lung cancer cell lines (A549, H2170, H1781, H460, H1993 and HCC4006) and non-cancerous immortalized lung cell line (BEAS-2B) were analyzed for expression of the indicated genes by quantitative real-time PCR. TBP was used as a control for calibration of the assessment. D, Protein expression levels of NFI family in several lung cancer cell lines (A549, H2170, H1781, H460, H1993 and HCC4006) and non-cancerous immortalized lung cell line (BEAS-2B) were examined by western blotting. E, F, Cellular migration (E) and invasion (F) were assessed in A549 cells with overexpression of GFP or NFI family genes that were treated or not treated with 100 ng/ml of S100A8/A9 for 12 h. Data are means ± SD, $^{*}P < 0.05$, $^{**}P < 0.01$ and $^{***}P < 0.001$. [Color figure can be viewed at wileyonlinelibrary.com]

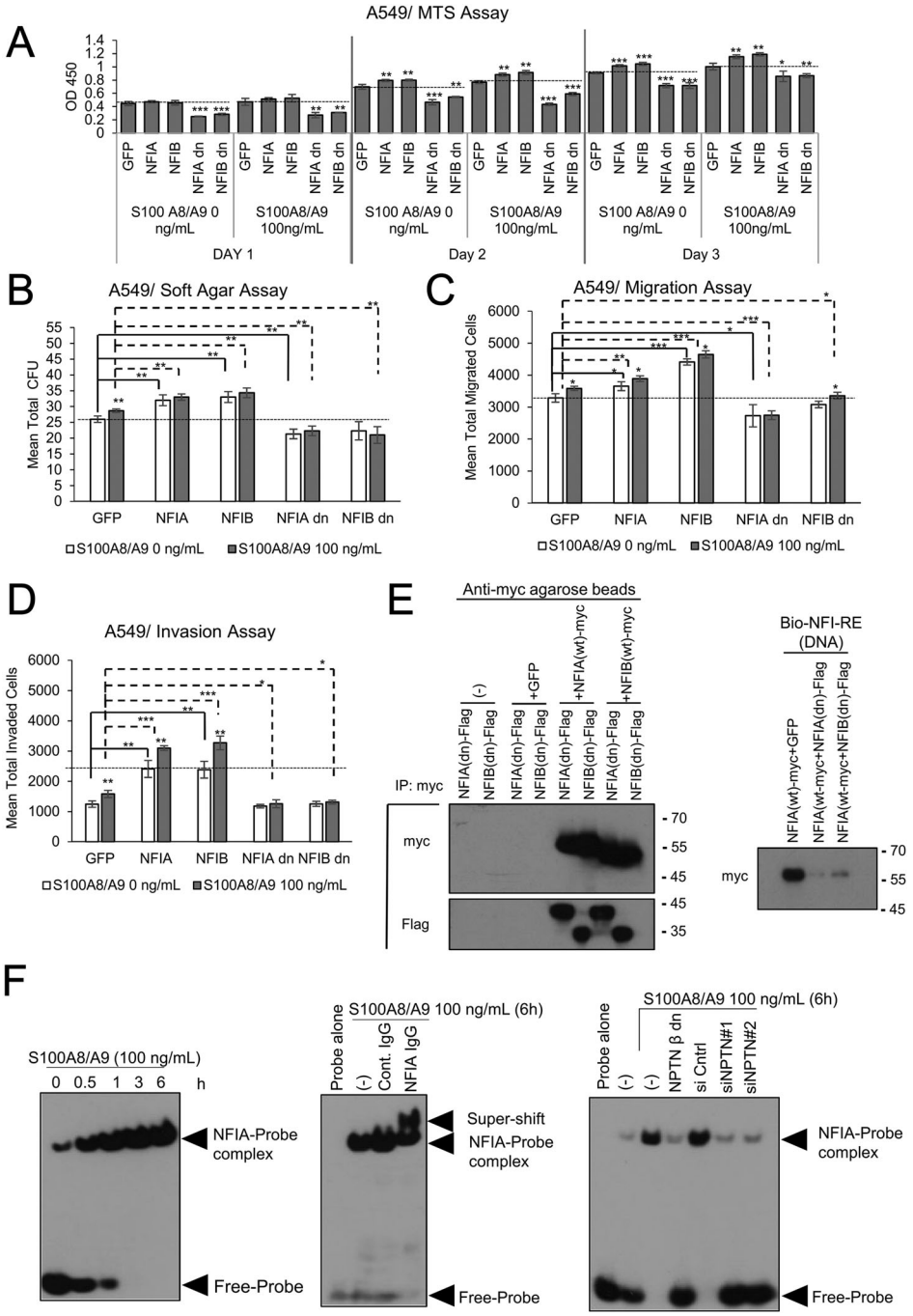

FIGURE 4 Critical function of NFIA and NFIB in S100A8/A9-NPTNβ-mediated cellular events. A, B, C, D, Simple growth (A), anchorage-independent growth (B), migration (C) and invasion (D) were evaluated in A549 cells with overexpression of wild or DNA-binding domain-lacking (DN) NFIA and NFIB by the MTS assay, spheroid counting assay, and Boyden chamber-based migration and invasion assays, respectively. The concentrations of S100A8/A9, for stimulation in the experiments (A) through (D) were all at 100 ng/mL and treatment periods were one, two and three days for the MTS assay (A), two weeks for the spheroid assay (B) and 12 h for the migration (C) and invasion (D) assays. Data from A through D are means ± SD, $^{*}P < 0.05$, $^{**}P < 0.01$ and $^{***}P < 0.001$. E, Analysis of homodimerization of NFIA/NFIA and NFIB/NFIB, and of heterodimerization of NFIA/NFIB. HEK293T cells were transfected with the indicated gene combinations, lysed and subjected to pull-down assay using anti-myc agarose beads (left panel) or streptavidin beads with biotin-conjugated NFI targeting DNA oligonucleotide (Bio-NFI-RE) (right panel). F, Electrophoretic mobility shift assay (EMSA) was performed in nuclear extracts prepared from A549 cells with a double-stranded oligonucleotide probe specific for NFI binding. A549 cells were stimulated with 100 ng/mL of S100A8/A9 for regular time intervals as indicated in the left panel. NFIA-specific binding was confirmed by super-shift assessment using NFIA IgG (middle panel). NFIA activation was evaluated after transfection of A549 cells with either the NPTNβ dn plasmid or two kinds of NPTN siRNA (siNPTN#1 and siNPTN#2) and subsequent stimulation with S100A8/A9 (100 ng/mL) for 6 h. [Color figure can be viewed at wileyonlinelibrary.com]

UNKNOWN. Among these genes, we focused on genes with altered expression that are associated with CANCER (Figure S7B, left) and METABOLIC (Figure S7B, right) in the disease category. According to the appearance of a series of genes enriched in these diseases, we particularly focused on renowned genes in red color (Figures S7B and S7C), which have been reported to be involved in either cancer progression or suppression (Figure S7C). The expression of the listed genes was confirmed by quantitative real-time PCR analysis (Figure 5A). The expression of the genes in the indicated cells provided more detailed information on their expression regulation in either a positive manner (IDH1, ASS1, KLF4, KLF13, SPDEF and ID4) or negative manner (THBS1 and DKK1). To select more suitable genes regulated by the signaling pathway through the NPTNβ-NFIA/NFIB axis, we focused on IDH1, KLF13, SPDEF and DKK1. Among these genes, we designated SPDEF and KLF13 as representative target genes for which expression is significantly regulated by the identified signaling axis. Although the regulation of ASS1 and THBS1 expression is not obvious, it seems that the expression of both KLF4 and ID4 is positively regulated by NFIA/NFIB without NPTNβ. Since SPDEF has a more critical role than that of KLF13 in cancer progression, we decided to focus on SPDEF and examined the expression of SPDEF at protein level in several lung cancer cells lines. We found that the SPDEF was consistently and significantly higher in lung cancer cell lines (A549, H2170, H1781, H460, H1993 and HCC4006) than that in non-cancerous BEAS-2B cell line (Figure 5B). Next, we examined the functions of SPDEF through the S100A8/A9-NPTNβ-NFIA/NFIB axis. Result of cell-based assays including assays for anchorage-independent growth (Figure 5C), migration (Figure 5D) and invasion (Figure 5E) showed that SPDEF tended to be involved in acceleration of these cancer-related behaviors, especially in spheroidal proliferation, mediated by the S100A8/A9-NPTNβ-NFIA/NFIB axis. These results were further supported by the knockdown experiments using the SPDEF siRNAs in A549 NPTNβ wt stable clone (Figure S8A-S8D). From these results, we speculated that SPDEF and several other factors, including KLF13, IDH1 and DKK1, that are regulated by the S100A8/A9-NPTNβ-NFIA/NFIB axis cooperatively functions to provide cancer cells with a driving force for cancer progression. In our ongoing study, we will try to further uncover this unidentified orchestration of signal pathways at molecular levels.

3.5 | Activation of NFIA by TRAF2 and RAS signaling that leads to S100A8/A9-NPTNβ-induced upregulation of cellular spheroidal growth, migration and invasion

We recently reported that NPTNβ has at least two important adaptors, GRB2 and TRAF2, for its onset of downstream signaling (Figure 6A).[12] GRB2 activates RAS, by which multiple cancer-associated cellular events involved in the promotion of cell growth and survival are triggered. However, KRAS is already mutated to a constitutively active type in A549 cells. In addition, other lung cancer-associated oncogenes including EGFR and ERBB2 are linked to RAS activation.[17,18] We therefore examined the significance of the pathway through TRAF2 in the S100A8/A9-NPTNβ axis in A549 cells for cancer progression, to which NFIA may contribute at downstream. At first, we confirmed by immunoprecipitation that NPTNβ binds with TRAF2 at cytoplasmic tail but not with NFIA (Figure 6B). To inhibit either TRAF2 or RAS function, we used forced expression of TRAF2 dn or chemical inhibitors. By this approach, we found that S100A8/A9-mediated upregulation of NFIA (Figure 6C), scaffold-independent spheroid formation (Figure 6D), migration (Figure 6E) and invasion (Figure 6F) were all impaired by TRAF2 dn at significant levels and by a pan-RAS inhibitor (FTS) at moderate levels respectively. On the other hand, a KRAS-specific inhibitor had no appreciable suppressive effect (Figures 6D-6F) even at a 10-fold higher dose used in another experiment (data not shown). We also found that the suppressive effects of TRAF2 dn were further enhanced by the addition of the pan-RAS inhibitor (Figures 6C, 6E, and 6F). These results indicate an unusual role of TRAF2 as a signal transducer from NPTNβ to distant NFIA in activation and in cellular events such as anchorage-independent growth and invasive motility and that TRAF2 orchestrates with another RAS without KRAS to regulate these cellular events under S100A8/A9-NPTNβ downstream.

3.6 | NFIA/NFIB activation through the S100A8/A9-NPTNβ axis plays a critical role in lung cancer progression

To further analyze the relevance of the identified pathway from cell surface NPTNβ through TFs, NFIA and NFIB in an in vivo tumor metastasis model, we used A549 cell-derived stable transformant sublines (NPTNβ wt clone #11, NPTNβ wt + NFIA wt + NFIB wt clone #12, NPTNβ wt + NFIA dn + NFIB dn clone #2) and we performed direct pulmonary injection of the representative clones into immunocompromised nude mice and investigated the behaviors of transplanted cells in lung tissue (Figure 7A). We observed large tumor nodule composed of NPTNβ wt + NFIA wt + NFIB wt clone #12, which significantly different from NPTNβ wt clone #11 and NPTNβ wt + NFIA dn + NFIB dn clone #2. Interestingly, aggressive dissemination was observed in the tumor front of NPTNβ wt + NFIA wt + NFIB wt clone #12 (Figure 7B). However, distant metastasis to other organs such as the liver and brain was not observed during the experimental period even in the case of NPTNβ wt + NFIA wt + NFIB wt clone #12 (data not shown). These phenomena were also confirmed by the same experiments using other clones (Figure S9). To determine whether tumor size is dependent on growth activity, we next attempted to immunostain Ki-67. In this evaluation, tumors were detected by cytokeratin eight staining, and there was a notable difference of Ki-67-positive cells among the tumors (Figure 7C), that is, there were significant increases in the number and staining intensity of Ki-67-positive cells in the NPTNβ wt + NFIA wt + NFIB wt clone #12-derived tumor (Figure 7D). The results indicated that there is a strong relationship between tumor size (cytokeratin 8) and growth activity (Ki-67) in tumors derived from the clones. Taken together, the results indicate that the NPTNβ-NFIA/NFIB axis in lung cancer contributes to disseminative growth of the cancer within the originated lung area through stimulation of the cancer NPTNβ-NFIA/NFIB axis upon binding with S100A8/A9, which is supplied by the lung stroma surrounding the tumor.

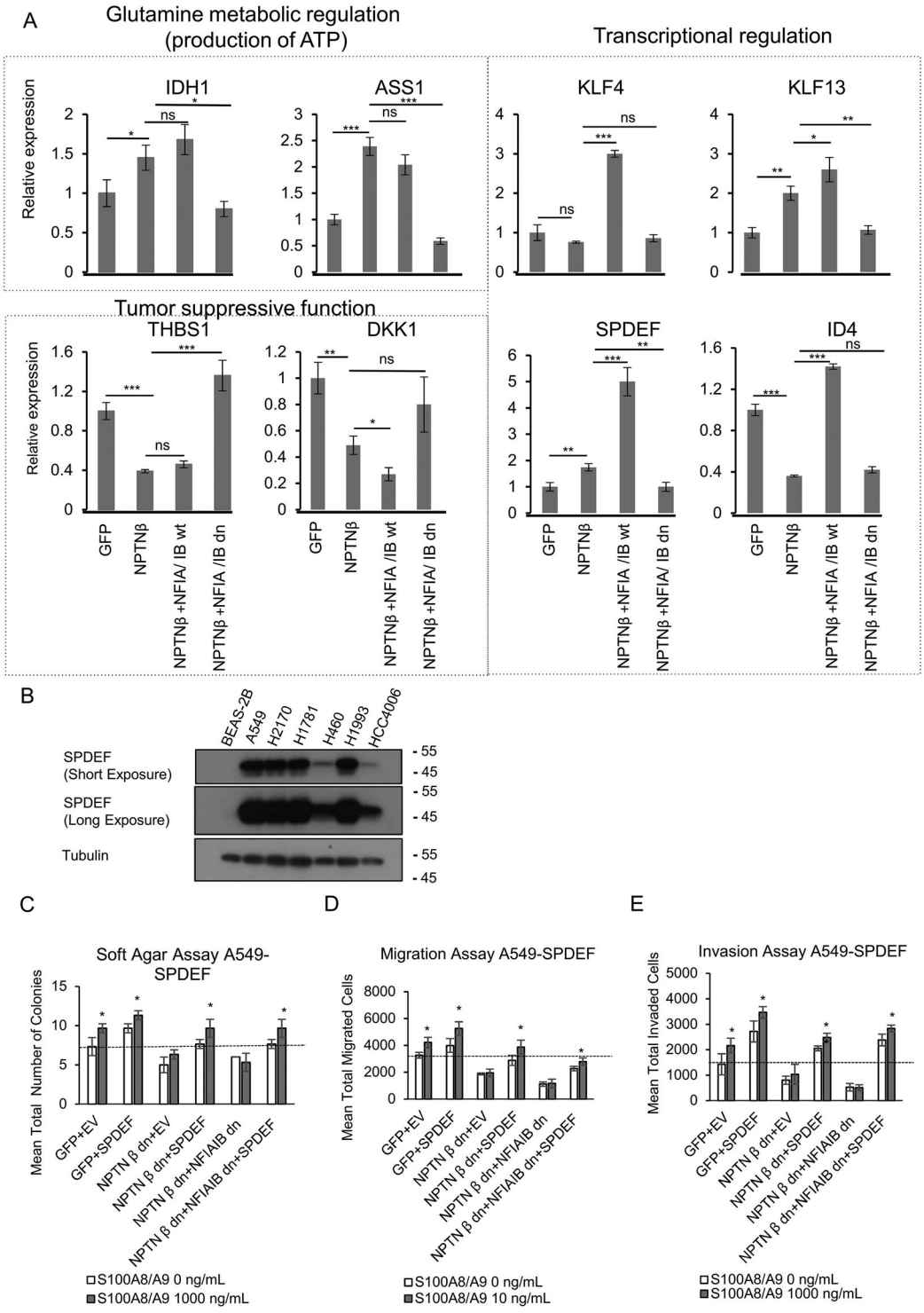

FIGURE 5 NFIA/NFIB-mediated induction of SPDEF promotes cellular anchorage-independent growth, migration and invasion. A, Quantitative real-time PCR analysis was done in A549 cell clones for the indicated genes. Total RNAs were prepared from clones (GFP, NPTNβ wt clone #11, NPTNβ wt + NFIA wt + NFIB wt clone #12, NPTNβ wt + NFIA dn + NFIB dn clone #2). The expression level in each sample was shown after calibration with the TBP value. B, SPDEF expression at protein level was examined by western blotting for several lung cancer cells (A549, H2170, H1781, H460, H1993 and HCC4006) and non-cancerous immortalized BEAS-2B cells. C, D, E, Anchorage-independent growth (C), migration (D) and invasion (E) were evaluated in A549 cells with transfection of the indicated vectors (GFP + Empty (ev), GFP + SPDEF, NPTNβ dn + ev, NPTNβ dn + SPDEF, NPTNβ dn + NFIA dn + NFIB dn, NPTNβ dn + NFIA dn + NFIB dn + SPDEF) by the spheroid counting assay and Boyden chamber-based migration and invasion assays, respectively. The concentrations of S100A8/A9 for stimulation in experiments (C) through (E) were 10 ng/ml for migration, 1000 ng/mL for invasion and spheroid assay, and treatment periods were two weeks for the spheroid assay (C) and 12 h for the migration (D) and invasion (E) assays. Data from A through E are means ± SD, $^{*}P < 0.05$, $^{**}P < 0.01$ and $^{***}P < 0.001$. [Color figure can be viewed at wileyonlinelibrary.com]

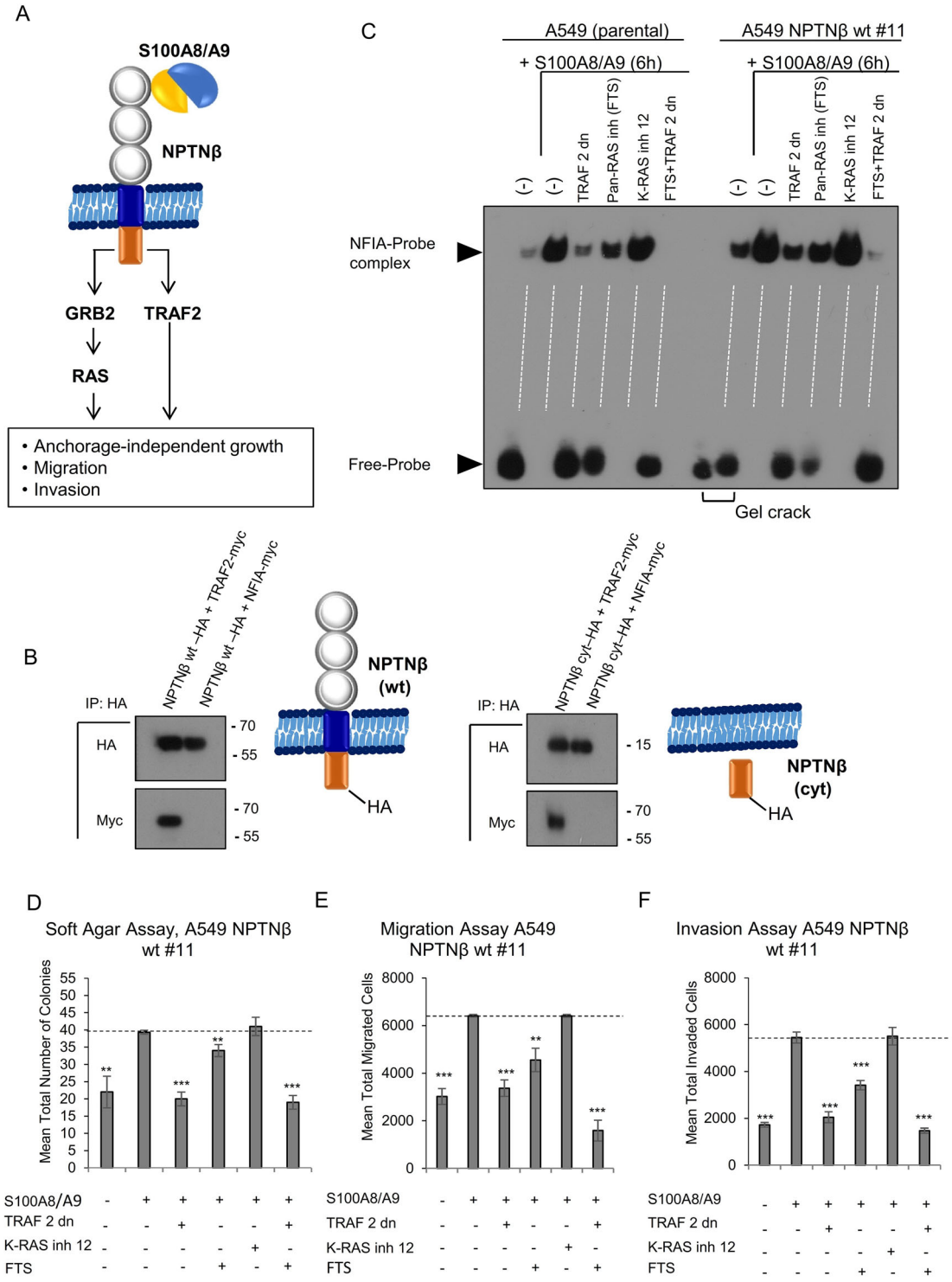

FIGURE 6 Activation of NFIA by TRAF2 and RAS signaling that leads to S100A8/A9-NPTNβ-induced cellular spheroid formation, migration and invasion. A, Schematic drawing of NPTNβ downstream pathway. B, Evaluation of the binding between NPTNβ and TRAF2 or NPTNβ and NFIA by immunoprecipitation. HEK293T cells were transfected with the indicated gene combinations, lysed and subjected to pull-down assay using anti-HA agarose beads. In this experiment, full-length of NPTNβ (wt) (left panel) and its cytoplasmic domain (cyt) (right panel) were used for immunoprecipitation targets. C, NFIA activation was evaluated by EMSA in A549 cells with TRAF2 dn overexpression, KRAS inhibitor (KRASI) treatment, non-selective RAS inhibitor (pan-RASI) treatment, or treatment with a combination of TRAF2 dn and pan-RASI. D, E, F, Anchorage-independent growth (D), migration (E) and invasion (F) were evaluated in A549 cells under the same conditions as those in (B). The concentrations of S100A8/A9 for stimulation in the experiments (D) through (F) were all 100 ng/ml and treatment periods were two weeks for the spheroid assay (D) and 12 h for the migration (E) and invasion (F) assays. Data from D through F are means ± SD, $^{*}P < 0.05$, $^{**}P < 0.01$ and $^{***}P < 0.001$. [Color figure can be viewed at wileyonlinelibrary.com]

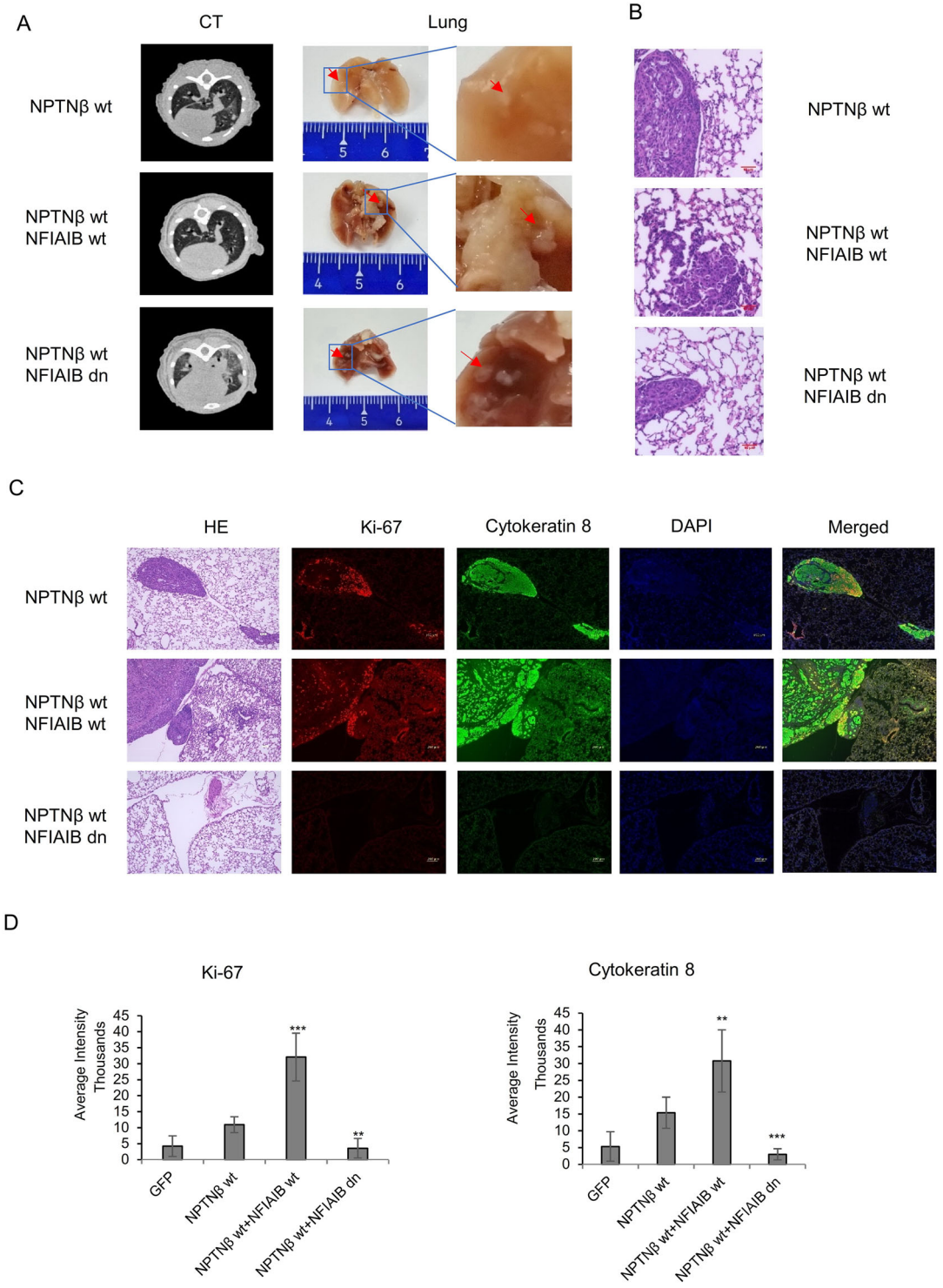

FIGURE 7 NFIA/NFIB activation through the S100A8/A9-NPTNβ axis is important for lung cancer disseminating progression. A549 cell-based stable trasnformants, GFP, NPTNβ wt #11, NPTNβ wt + NFIA wt + NFIB wt #12, and NPTNβ wt+ NFIA dn + NFIB dn #2 (all 5×10^5 cells) were injected into the lungs of mice and maintained for one month. A, Representative photographs of the transplanted cell-derived tumors in mice (computed tomography (CT) image: left) and dissected whole lungs (right). Tumors are shown by arrows. B, Hematoxylin and eosin (H&E) staining was done in the tumor nodules in the lung. Images were focused on tumor rims. C, Immunohistochemistry for Ki-67, cytokeratin 8 and DAPI was done in the indicated clone-derived tumor sections. D, Quantification of the intensities of Ki-67 and cytokeratin 8 staining was performed. Data are means ± SD, $^{**}P < 0.01$ and $^{***}P < 0.001$. [Color figure can be viewed at wileyonlinelibrary.com]

4 | DISCUSSION

The results of our study showed that extracellular S100A8/A9 induced by cancer-associated inflammation in the lung plays a pivotal role in lung cancer progression through enhanced anchorage-independent growth, migration and invasion. For effectively receiving the S100A8/A9 signal, lung cancer cells use their cell surface NPTNβ that which is highly elevated at both mRNA and protein levels. Upon binding of S100A8/A9 to NPTNβ, the TRAF2 adaptor molecule induce all the above-mentioned cellular events via NFIA/IB, resulting in cancer progression.

We first showed that NPTNβ acts as one of the S100A8/A9 receptors in keratinocytes.[12] When keratinocytes are in legion of an inflammatory skin disease such as atopic dermatitis, extracellular S100A8/A9 induced by inflammation stimulates NPTNβ in keratinocytes, leading to the acquisition of much higher potential for proliferation and production of cytokines and chemokines in the stimulated keratinocytes, linking to skin hyperplasia with serious inflammation.[12] Because NPTNβ has at least two adaptor molecules, GRB2 and TRAF2,[12] which are known to activate RAS-mediated ERK[12,18] and NFκB,[12,19,20] eventually possible to link proliferation and inflammation, respectively. The pathways that were mediated by these adaptor molecules (GRB2-RAS pathway and TRAF pathway) might also have link to NFIA/NFIB activation and NPTNβ upon S100A8/A9 binding, lead to lung cancer progression. In lung A549 cancer cells, significant cellular events associated with the S100A8/A9-NPTNβ axis were cellular motility, invasiveness and anchorage-independent growth. In this study, we found that the TRAF2 pathway is more important than the GRB2-RAS pathway, since RAS is already in a state of sustained activation in A549 cells owing to a constitutively active KRAS mutation.[19,20] Furthermore, overexpression and constitutive active mutations of EGFR and ERBB2, which are critical for carcinogenesis and subsequent progression of lung cancers, are all linked to downstream RAS activation.[17,18] As expected, we found that TRAF2 through NPTNβ triggered by S100A8/A9 binding was important lung cancer progression in culture system (Figure 6). We also found that TRAF2 cooperatively functions with another RAS without KRAS. To know the importance of another RAS in lung cancer cells, we examined the expression of RAS family genes in cancer cells. The results showed that two RAS family genes, RAS-Like Family 11 Member A (RASL11A) and Embryonic Stem Cell-Expressed Ras (ERAS), were highly upregulated in A549 cells and all other lung cancer cells that were examined (Figure S10). These findings may provide a clue for determining the role of other RAS family genes in the GRB2 pathway regulated by the S100A8/A9-NPTNβ axis in lung cancer (Figure 6A).

We also have investigated how TRAF2 contributes to NFIA and NFIB activation. NFIs' regulation is still in enigma in many parts; however, Lee et al showed that there is feed-forward regulation between NFκB and NFIA.[21] Thus, TRAF2 may indirectly activate NFIA through activation of NFκB. In addition, NFIA is able to function as a heterodimer with NFIB,[22–24] which may be the reason why we found functional similarity between NFIA and NFIB in our experimental settings. In fact, our immunoprecipitation (Figure 4E left panel) showed that NFIA and NFIB can form not only homodimer by each itself (NFIA/NFIA, NFIB/NFIB) but also heterodimer (NFIA/NFIB). The homodimer or heterodimer formation is probably required for an active function of NFIA and NFIB since both inclusions of dominant negative NFIA and NFIB to the wild type NFIA effectively removed the DNA-binding ability of NFIA (Figure 4E right panel).

Once NFIA/NFIB had been activated, it enhanced anchorage-independent growth, cellular motility and invasiveness in lung cancer cells (Figure S6). Interestingly, these cellular events were followed by a notable change in cell shape toward a stromal phenotype (Figure S5B), which may indicate an epithelial-mesenchymal transition (EMT).[25,26] We were therefore interested in EMT genes, which should show altered expression at significant levels in NFIA/NFIB wt and its non-functional dn type, but contrary to our expectations, no notable changes in the expression of genes related to EMT were detected in subsequent studies using RNA sequence-based analysis (Figure S7). Instead, many cancer-associated genes were enriched in the condition of sustained overexpression of NFIA/NFIB. We found that one of the candidates, SPDEF, was involved in part in anchorage-independent growth, cellular motility and invasiveness in lung cancer cells (Figures 5C-5E and Figure S8), suggesting that SPDEF coordinately functions with other molecules (Figure S7) under NFIA/NFIB to lead cancer-associated cellular events that may also be linked to the appearance of an EMT-like cellular phenotype. Interestingly, SPDEF has an inverse function for cancer progression. Consistent with our results obtained in lung cancer cells, GEPIA public database (http://gepia.cancer-pku.cn/detail.php?gene=SPDEF) provided much higher expression of SPDEF in lung tumors than those in normal lung tissues (data not shown) that links well a consistent increase in NFIA in the lung tumors compared with their adjacent normal tissues in lung cancer patients.[27] A high expression level of SPDEF in estrogen receptor-positive breast tumors showed a significant correlation with poor overall survival. In addition, Mukhopadhyay et al reported that SPDEF-CEACAM6 is a highly active oncogenic axis in breast cancer.[28] On the other hand, some studies showed that SPDEF represses tumorigenesis, EMT and metastasis in prostate cancer cells, suggesting the presence of an unusual complex mechanism of SPDEF regulation dependent on cancer type.[29–32]

Finally, we discuss about how S100A8/A9 is induced in the lung in which lung cancer cells reside in. The result of immunohistochemistry showed that S100A8/A9 was produced and secreted by either stroma cells surrounding cancer cells or by cancer cell themselves. Interestingly, Hoshino et al reported that tumor-derived exosomes induce the expressions of multiple *S100* genes, including S100A4, A6, A10, A11, A13 and A16, in normal fibroblasts in the lung when the exosomes bind to and are incorporated into the fibroblasts.[33] On the other hand, the main sources of S100A8/A9 secretion have been shown to be inflammatory monocytes[2] and neutrophils,[2,4,5] which exist in the stroma around cancer cells in the lung. Thus, it possible that lung cancer-derived exosomes induce S100A8/A9 in these cells in the lung in accordance with the results reported by Hoshino et al. In fact, our results showed that lung cancer-derived exosomes stimulate S100A8/A9 secretion, leading to cancer cell migration and invasion at critical levels (Figure S11). Regarding this, Hoshino et al also showed that cancer-mediated exosomes induce S100A8 from Kupffer cells in the liver, which may attract cancer cells.[33] We hence speculate that NPTNβ wt + NFIA wt + NFIB wt clone #12 may be attracted to the liver through sensing

S100A8 since NPTNβ can recognize S100A8. To enable this phenomenon, intrinsic abundant NFIA/NFIB may be additively required. Future studies will uncover these complex mechanisms.

In this study, we did not explore the importance of S100A8/A9 as a potential biomarker for lung cancers. Some studies have been reported that S100A8/A9 is detectable at significant levels in plasma in patients who burdened several types of cancers including renal cell cancers,[34] colorectal cancers,[35] prostate cancers[36] and pancreatic ductal adenocarcinomas (PDACs),[37] which sets conditions of malignant cancers apart from those of non-cancerous inflammatory diseases. Thus, we are expecting that S100A8/A9 may also be a useful biomarker in lung cancers.

Our findings indicate that S100A8/A9-NPTNβ plays a pivotal role in lung cancer progression with dissemination through a significant pathway, especially through TRAF2-NFIA/NFIB signaling. The pathway may coordinately function with other key oncogenic pathways triggered by EGFR, ERBB2, KRAS, and so on for the process of aggressive growth and metastasis of lung cancer (Figure 8). We hence believe that strategies targeting S100A8/A9-NPTNβ may effectively block lung cancer progression and that such approaches will be useful when combine with the established common chemotherapy.

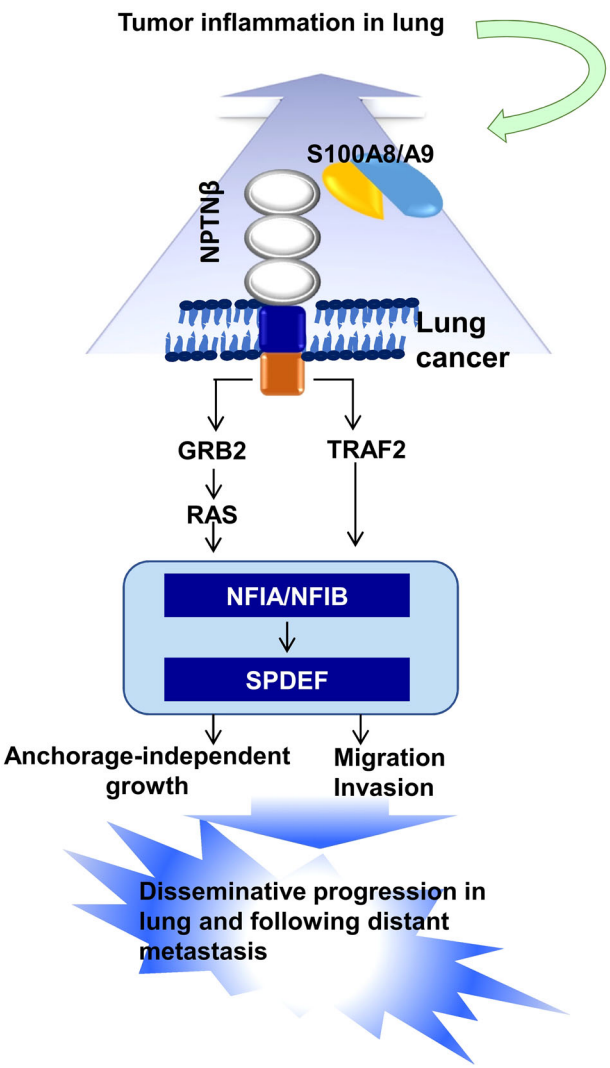

FIGURE 8 Schematic pathways of S100A8/A9-NPTNβ-induced disseminative progression of lung cancer. [Color figure can be viewed at wileyonlinelibrary.com]

ETHICS APPROVAL AND CONSENT TO PARTICIPATE

The studies using patient-derived tissue sections for immunohistochemistry were approved by the research ethics committees of Niigata University Medical and Dental Hospital. Written informed consent was obtained from each patient for use of the materials. All animal experimental protocols were approved by the Animal Experiment Committee in Okayama University (approval No. OKU-2014011). All mouse procedures and euthanasia, including cell transplantations, were done painlessly or under anesthesia within the strict guidelines of the Experimental Animal Committee of Okayama University.

AUTHORS' CONTRIBUTIONS

WS, HM, and MS were involved in conceptual guidance and data interpretation. IWS and MS wrote the manuscript. IWS performed in vitro experiments and WB. MS performed plasmid DNA construction, EMSA and WB. RK performed bioinformatics analysis of RNAseq data and protein purification. IWS, NT, and HS performed animal study. YI and ST performed RT-PCR and RNA seq analysis. EK provided clinical samples and performed IHC. JF, HM, RK and KiY prepared the S100A8/A9 recombinant protein. AY, KS, HY and JS prepared and performed HE staining of the animal tissue. YC, IMW, and EWP performed the confirmation of the in vitro experimental results. ST, TH and MN provided a critical review of the manuscript. MS proposed and supervised the study. All authors read and approved the manuscript.

ACKNOWLEDGMENTS

This research was supported in part by the Project for Cancer Research and Therapeutic Evolution (P-CREATE) from the Japan Agency for Medical Research and Development (AMED, Grant Number JP17cm0106216) to MS., JSPS KAKENHI (Grant Number 17H03577) to MS., Takeda Science Foundation to MS., Princess Takamatsu Cancer Research Fund to MS., Kobayashi Foundation for Cancer Research to MS., and Fujii Memorial Medical Science Foundation to MS.

CONFLICT OF INTEREST

The authors declare that they have no conflicts of interest with the contents of this article.

ORCID

Masakiyo Sakaguchi http://orcid.org/0000-0002-0566-4872

REFERENCES

1. Siegel RL, Miller KD, Jemal A. Cancer statistics, 2016. *CA Cancer J Clin*. 2016;66:7–30.
2. Srivastava MK, Anderson A, Zhu L, et al. Myeloid suppressor cells and immune modulation in lung cancer. *Immunotherapy*. 2012;4:291–304.
3. Srikrishna G. S100A8 and S100A9: new insights into their roles in malignancy. *J Innate Immun*. 2012;4:31–40.
4. Vogl T, Tebrock K, Ludwig S, et al. Mrp8 and Mrp14 are endogenous activators of Toll-like receptor 4, promoting lethal, endotoxin-induced shock. *Nat Med*. 2007;13:1042–1049.
5. Ma L, Sung P, Zhang J-C, Zhang Q, Yao S-H. Proinflammatory effects of S100A8/A9 via TLR4 and RAGE signaling pathways in BV-2 microglial cell. *Intern J Mol Med*. 2017;40:31–38.
6. Ichikawa M, Williams R, Wang L, Vogl T, Srikrishna G. S100A8/A9 activate key genes and pathways in colon tumor progression. *Mol Cancer Res*. 2011;9:133–148.
7. Sakaguchi M, Murata H, Yamamoto K-I, et al. TIRAP an adaptor protein for TLR2/4, transduces a signal from RAGE phosphorylated upon ligand binding. *PLoS ONE*. 2011;6:e23132.
8. Ghavami S, Rashedi I, Dattilo BM, et al. S100A8/A9 at low concentration promotes tumor cell growth via RAGE ligation and MAP kinase-dependent pathway. *J Leukoc Biol*. 2008;83:1484–1492.
9. Hibino T, Sakaguchi M, Miyamoto S, et al. S100A9 is a novel ligand of EMMPRIN that promotes melanoma metastasis. *Cancer Res*. 2012;73: 172–183.
10. Ruma IM, Putranto EW, Kondo E, et al. MCAM, as a novel receptor for S100A8/A9, mediates progression of malignant melanoma through prominent activation of NF-κB and ROS formation upon ligand binding. *Clin Exp Metastasis*. 2016;33:609–627.
11. Sumardika IW, Youyi C, Kondo E, et al. β-1,3-galactosyl-O-glycosyl-glycoprotein β-1,6-N-acetylglucosaminyltransferase 3 increases MCAM stability, which enhances S100A8/A9-Mediated cancer motility. *Onco Res*. 2018;26:431–444.
12. Sakaguchi M, Yamamoto M, Miyai M, et al. Identification of an S100A8 receptor Neuroplastin-β and its heterodimer formation with EMMPRIN. *J Inv Dermatol*. 2016;136:2240–2250.
13. Ortiz ML, Lu L, Ramachandran I, Gabrilovich DI. Myeloid-derived suppressor cells in the development of lung cancer. *Cancer Immunol Res*. 2013;2:50–58.
14. Sakaguchi M, Watanabe M, Kinoshita R, et al. Dramatic increase in expression of a transgene by insertion of promoters downstream of the cargo gene. *Mol Biotechnol*. 2014;56:621–630.
15. Chitale D, Gong Y, Taylor BS, et al. An integrated genomic analysis of lung cancer reveals loss of DUSP4 in EGFR-mutant tumors. *Oncogene*. 2009;28:2773–2783.
16. Aguirre-Gamboa R, Gomez-Rueda H, Martínez-Ledesma E, et al. SurvExpress: an online biomarker validation tool and database for cancer gene expression data using survival analysis. *PLoS ONE*. 2013;8:e74250.
17. Luo SY, Lam DCL. Oncogenic driver mutations in lung cancer. *Transl Respir Med*. 2013;1:6.
18. Berger AH, Imielinski M, Duke F, et al. Oncogenic RIT1 mutaions in lung adenocarcinoma. *Oncogene*. 2014;33:4418–4423.
19. Langsch S, Baumgartner U, Haemmig S, et al. MiR-29b mediates NF-kB signaling in KRAS-Induced non-Small cell lung cancers. *Cancer Res*. 2016;76:4160–4169.
20. Yang L, Zhou Y, Li Y, et al. Mutations of p53 and KRAS activate NF-kappaB to promote chemoresistance and tumorigenesis via dysregulation of cell cycle and suppression of apoptosis in lung cancer cells. *Cancer Lett*. 2015;357:520–526.
21. Lee JS, Hoxha E, Song HR. A novel NFIA-NFκB feed-forward loop contributes to glioblastoma cell survival. *Neuro-Oncology*. 2017;19:524–534.
22. Grabowska MM, Elliott AD, DeGraff DJ, et al. NFI transcription factors interact with FOXA1 to regulate prostate-specific gene expression. *Mol Endocrinol*. 2014;28:949–964.
23. Kruse U, Sippel AE. Transcription factor nuclear factor I proteins form stable homo- and heterodimers. *FEBS Lett*. 1994;348:46–50.
24. Chaudhry AZ, Lyons GE, Gronostajski RM. Expression patterns of the four nuclear factor I genes during mouse embryogenesis indicate a potential role in development. *Dev Dyn*. 1997;208:313–325.
25. Heerboth S, Housman G, Leary M, et al. EMT and tumor metastasis. *Clin Transl Med*. 2015;4:6.
26. Katz E, Dubois-Marshall S, Sims AH, et al. An in vitro model that recapitulates the epithelial to mesenchymal transition (EMT) in human breast cancer. *PLoS ONE*. 2011;6:e17083.
27. Tian X, Tian J, Tang X, et al. Particulate ß-glucan regulates the immunosuppression of granulocytic myeloid-derived suppressor cells by inhibiting NFIA expression. *OncoImmunology*. 2015;4:e1038687.
28. Mukhopadhyay A, Khoury T, Stein L, Shrikant P, Sood AK. Prostate derived Ets transcription factor and Carcinoembryonic antigen related cell adhesion molecule 6 constitute a highly active oncogenic axis in breast cancer. *Oncotarget*. 2013;4:610–621.
29. Steffan JJ, Koul S, Meacham RB, Koul HK. The transcription factor SPDEF suppresses prostate tumor metastasis. *J Biol Chem*. 2012;287: 29968–29978.
30. Cheng X-H, Black M, Ustiyan V, et al. SPDEF inhibits prostate carcinogenesis by disrupting a positive feedback loop in regulation of the foxm1 oncogene. *PLoS Genet*. 2014;10:e1004656.
31. Tamura RE, Paccez JD, Duncan KC, et al. GADD45α and γ interaction with CDK11p58 regulates SPDEF protein stability and SPDEF-mediated effects on cancer cell migration. *Oncotarget*. 2016;7: 13865–13879.
32. Gu X, Zerbini LF, Otu HH, Bhasin M, Yang Q, Joseph MG. Reduced PDEF expression increases invasion and expression of mesenchymal genes in prostate cancer cells. *Cancer Res*. 2007;67:4219–4226.
33. Hoshino A, Costa-Silva B, Shen TL, et al. Tumour exosome integrins determine organotropic metastasis. *Nature*. 2015;527:329–335.
34. Zhang L, Jiang H, Xu G, et al. Proteins S100A8 and S100A9 are potential biomarkers for renal cell carcinoma in the early stages: results from a proteomic study integrated with bioinformatics analysis. *Mol Med Rep*. 2015;11:4093–4100.
35. Kim H-J, Kang HJ, Lee H, et al. Identification of S100A8 and S100A9 as serological markers for colorectal cancer. *J Proteome Res*. 2009;8: 1368–1379.
36. Hermani A, Hess J, de Servi B, et al. Calcium-binding proteins S100A8 and S100A9 as novel diagnostic markers in human prostate cancer. *Clin Cancer Res*. 2005;11:5146–5152.
37. El Gammal AT, Sturm JH, Pinnschmidt HO, et al. Protein S100A8/A9: a potential new biomarker for pancreatic diseases. *Int J Clin Endocrinol Metab*. 2017;3:023–028.

How to cite this article: Sumardika IW, Chen Y, Tomonobu N, et al. Neuroplastin-β mediates S100A8/A9-induced lung cancer disseminative progression. *Molecular Carcinogenesis*. 2019;1–16. https://doi.org/10.1002/mc.22987